EVS29 Symposium
Montréal, Québec, Canada, June 19-22, 2016

Low Temperature Performance of Lithium-ion Batteries for Different Drive Cycles

Yashraj Tripathy[1], Andrew McGordon[1], John Low[1] and James Marco[1]

[1] *WMG, University of Warwick, Coventry, United Kingdom*

Abstract

Lithium-ion batteries, suitable for Battery-electric vehicles (BEVs) due to their high energy and power densities, and lifetime demonstrate deterioration in energy and power available at lower temperatures. It is attributed to reduction in capacity and increase in internal resistance. Investigations are carried out to determine energy, and power decline for four drive-cycles: FTP, NEDC, UDDS and US06. The minimum temperatures where the battery meets the drive-cycles' energy and power requirements are determined. The impact of regenerative-braking and self-heating on battery performance is discussed. The minimum temperature where any drive-cycle is met by the battery is directly proportional to its aggressiveness.

Keywords: Lithium Battery, BEV (Battery electric Vehicle), Power, Regenerative Braking, Internal Resistance

1 Introduction

Battery-electric vehicles (BEVs) are gaining prominence in providing solutions to the growing harms caused by the increasing number of vehicles on the environment [1]. As an Internal Combustion Engine (ICE) is the key component governing the efficiency and performance in a conventional vehicle; similarly in a BEV, it is the Energy Storage System (ESS) [2]. An important factor in BEVs becoming commonplace is the quality of its ESS [3]. An ideal ESS should have high energy and power density, excellent lifetime, and must be reliable for different C-rates and ambient temperatures [4]. Batteries have been widely adopted due to their high energy and power densities, compact size and reliability [2]. For batteries, the available energy is an indicator for the driving-range of the vehicle and the maximum charge/discharge C-rates point to power (acceleration and regenerative-braking) performance [5]. Although Lithium-ion batteries have become a major player in the BEV market, they suffer from severe power and energy losses at lower ambient temperatures [6, 7]. In colder countries such as Canada, Norway, etc., where the temperatures drop down to -30 ^{o}C, the benefits BEVs offer are offset by the effect of lower ambient temperatures [8]. It is primarily attributed to decline in the energy and power available from the battery at such temperatures [7, 8] and can be quantified as a

reduction in battery capacity, a lower maximum voltage (to avoid Lithium-plating [9]) and an increase in internal cell resistance [6, 10]. The effect is amplified at the higher C-rates that are expected in legislative and real-world drive-cycles. At lower temperatures due to a higher internal resistance, the cell/battery heats up faster [10]. This temperature rise (self-heating) has the potential to improve battery power performance, albeit at a loss of the available energy [11].

The aim of this paper is to quantify the deterioration in energy and power available from a Lithium-ion cell/battery at low temperature based on the change in battery capacity, voltage and internal resistance with ambient temperature. This affects the driving-range and performance of a BEV. The analysis has been carried out on four legislative drive-cycles such as UDDS, FTP, NEDC and US06. The paper comments on the impact of battery self-heating towards improving charge/discharge power and its subsequent impact on available energy.

2 Li-Ion Cell at Low Temperature: Energy and Power Decline

The energy available from a battery or cell is directly proportional to the corresponding capacity [10]. During either charge or discharge process, the rate at which voltage changes with capacity is higher at lower ambient temperatures [9]. This is due to increase in internal cellular resistance [12] associated with slower rate of chemical reactions taking place inside the cell [13].

Further, to prevent Lithium-plating, the maximum voltage that a cell can attain during charging is also lower at low temperatures [14]. The power capability of a cell is strongly affected by its internal resistance and SOC (dependent on the open-circuit voltage of the cell) [15]. Thus, the cell has limiting power capabilities (charge/discharge) at varying ambient temperatures and SOCs [16].

2.1 Capacity, Voltage and Internal Resistance

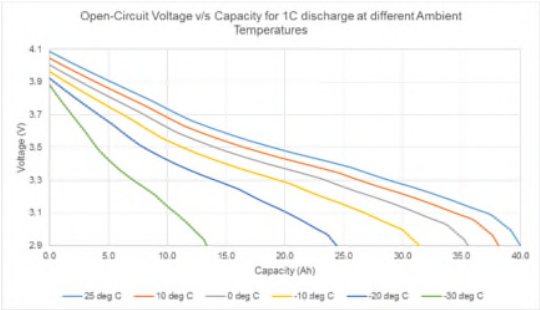

Figure 1. Voltage versus Capacity for 1C Discharge at Different Ambient Temperatures [1]

As seen in Fig. 1, for a 40 Ah Lithium Polymer cell, for a discharge current of 40 A, its discharge capacity declines from 40 Ah at 25 ^{o}C to ~35.5 Ah at 0 ^{o}C and eventually to ~13 Ah at -30 ^{o}C [6]. Apart from having an impact on the energy available from a cell/battery (voltage drops faster with capacity leading to a smaller area under the curve), a higher internal resistance at lower ambient temperature leads to lower power-capability. At a median SOC (50%) for discharge, it is seen in Fig. 2 that the internal resistance although invariable at higher ambient temperatures is twice the value at -30 ^{o}C (1.6 mΩ) as compared to at 25 ^{o}C (0.8 mΩ).

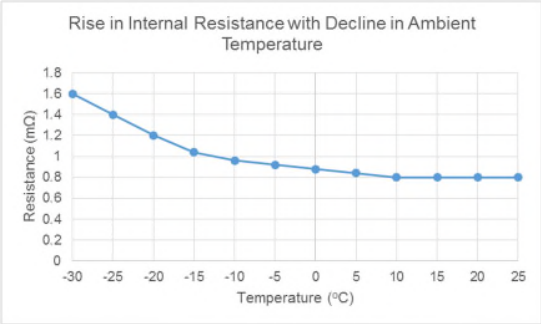

Figure 2. Increase in Internal Cell Resistance al Lower Ambient Temperatures (50% SOC) [1]

2.2 Energy and Power

The energy available from a cell/battery is defined as [10]:

$$E = \frac{V \int I dt}{3600} \tag{1}$$

Here, 'E' is the energy available from the cell at the end of a charge/discharge operation, 'V' is the voltage of the cell that is 3.7 V as advised by the manufacturer. 'I' is the instantaneous charge/discharge current for the cell. Since, the unit for the energy available from the cell is in Ampere-hour (Ah), the value on the right-hand-side is divided by 3600. This is based on Burke's equation for maximum charge/discharge power [15]:

$$P_{theoretical} = \eta\,(1-\eta)\,\frac{{V_{oc}}^2}{4R} \tag{2}$$

Here, '$P_{theoretical}$' the theoretical maximum charge/discharge power in kW, V_{oc} is the open-circuit voltage of the cell, 'R' is the internal cellular resistance. 'η' is the efficiency of the cell which to maximize the value for '$P_{theoretical}$' is taken as 0.5.

The cell cannot be discharged below the cut-off voltage (V_{min}) for a particular application (2.9 V in this case) and the maximum voltage (V_{max}) allowed during charging is limited by the BMS to avoid Lithium-plating at a particular temperature. Thus, from Fig. 1, Eqn. 2 is modified and actual Power (P_{actual}) is calculated as follows:

$$P_{actual} = \frac{{V_{oc}}^2 - {V_{lim}}^2}{4R} \tag{3}$$

Here, depending on whether the cell is charging or discharging, V_{lim} is V_{max} or V_{min} respectively. Also, charging power is taken as negative and discharging power as a positive value.

3 Methodology

The energy and power demanded by a BEV has been calculated using a backward-facing model. This has been carried out for four different legislative drive-cycles, viz. UDDS, FTP, NEDC and US06. The power-profiles have then been modified into current-profiles to analyze the energy and power deterioration at a cell level. Based on the formulae for available energy and maximum charge/discharge power, further analysis has been carried

out to find out the minimum temperatures at which the cell is able to meet the four drive-cycles both in terms of energy and power. Further, cell self-heating has also been included in the analysis to observe the impact it has on performance. Finally comments shall be made on allowing managed regenerative-braking at subzero temperatures and the need for a Supercapacitor-based HESS shall be evaluated.

3.1 Vehicle Model

From the speed (m/s) versus time (s) data available for different drive-cycles (UDDS, FTP, NEDC, and US06), the power-profile is created. The following equation presents the force required to meet a particular driving profile at every time-step (1s):

$$F = (m * a) + (0.5 * C_D * \rho * A * v^2) + (m * g * f_r) \quad (4)$$

Here 'F' is the force required per second by the vehicle 'v' is the instantaneous speed of the vehicle and 'a' is the instantaneous acceleration of the vehicle.

Gross Mass of the Vehicle, 'm' = 1945 kg, Coefficient of Drag, 'C_D' = 0.28, Density of Air, 'ρ' = 1.225 kg/m^3, Frontal Area of Vehicle, 'A' = 2.744 m^2, Gravitational Acceleration, 'g' = 9.81 m/s^2, Friction Coefficient,'f_r' = $0.01 * \left(1 + \frac{v}{576}\right)$.

The force values ensure that the wheels are rotating at a particular angular velocity (ω_w). Correspondingly, the required torque at the wheels (τ_w) is also calculated. Here, '*R*' is 0.316 m for a wheel (any) and the gear-box ratio (G) is 7.9377.

$$\omega_w = \frac{v}{R} \quad (5) \qquad \tau_w = F * R \quad (6)$$

Here R is the radii of the vehicle's wheels. Thus, using the gear-box ratio, the angular velocity and torque to be generated by the 75 kW AC Motor can be calculated. The following equations have been used:

$$\omega_{motor} = G * \omega_w \quad (7) \qquad \tau_{motor} = \frac{\tau_w}{G} \quad (8)$$

Here, τ_w and ω_w are the motor torque and motor angular-velocity respectively. Using the motor-efficiency map for the 75 kW AC Motor (Figure 3), the corresponding efficiencies (η) for charge and discharge loads were defined.

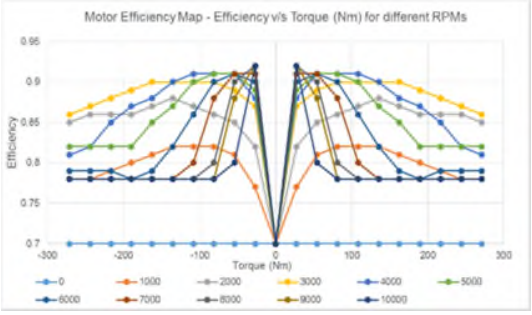

Figure 3. Motor Efficiency Map for 75 kW A/C Motor

Consequently, the power required and the power delivered (via regen-braking) every second from the battery is calculated. The total energy required from the battery is calculated by adding all the instantaneous powers (both charging and discharging) (Table 1). It has been assumed that the regenerative-braking efficiency (RE) is 100%. The energy required is that for a single drive-cycle.

Table 1. Drive Cycle Analysis at Vehicular Level

Drive Cycle	Energy (kWh)	Max Accel. (m/s^2)	Maximum Discharge Power (kW)	Max Decel. (m/s^2)	Maximum Charge Power (kW)
FTP	2.38	1.60	47.56	-1.47	-46.69
NEDC	1.71	1.06	52.25	-1.39	-27.08
UDDS	1.56	1.47	47.56	-1.47	-27.62
US06	2.62	3.73	133.68	-3.07	-55.10

3.2 Cell/Battery Model

The cell chosen has a Lithium Polymer chemistry, has a nominal voltage of 3.7 Volts and maximum and minimum operating voltages of 4.1 and 2.9 Volts respectively. It has a nominal capacity of 40 Ah. The pack voltage is 380 Volts and 106 cells are arranged in series. A Lithium Polymer chemistry has been chosen as it has one of the highest power densities amongst all Lithium chemistries [3]. The total energy available from the pack is 15.2 kWh at 25 ^oC. The temperature effects on cell parameters (capacity, maximum voltage and internal resistance) have been adopted as described in the previous sections. It has been assumed that even at lower temperatures, all energy available from regenerative-braking can be absorbed, depending upon the efficiency of the motor/generator. For quantifying the energy and power deterioration of the Lithium-ion cell, the energy and power requirements for different drive-cycles shown in Table 1 are scaled down to cell level considering a serial arrangement of cells (Table 2). The total energy available from a cell at 25 ^oC would be ~143.4 Wh.

Table 2. Drive Cycle Analysis at Cell Level

Drive Cycle	Energy (Wh)	D/C Power (W)	Charge Power (W)
FTP	22.46	448.68	-440.47
NEDC	16.14	492.93	-255.47
UDDS	14.72	448.68	-260.57
US06	24.72	1261.13	-519.81

3.3 Simulations

For energy considerations, it has been assumed that the cell/battery operates within SOC values of 75% and 25%. This entails roughly 71.7 Wh and 7.6 kWh of energy being correspondingly available from the cell or battery. Based on the power profiles for the different drive-cycles calculated and the temperature-dependent data available for the Lithium Polymer cell and Equation (3), a MATLAB/Simulink model has been designed to facilitate the present analysis. The model has the current-profile as an input to the temperature-dependent cell that calculates limiting charge/discharge power values based on Equation (3). Finally, the limiting power values offered by the cell for a particular drive-cycle are matched with the power demanded by that drive-cycle to find whether the cell can meet the power requirements of the drive-cycle. Also, based on the energy available from the cell at different temperatures; the energy demanded by the drive-cycle is compared to the energy available to find whether the battery is meeting the energy requirements of the drive-cycle. This analysis is carried out for the NEDC, FTP, UDDS and US06 drive-cycles. Further, based on the current-profile of a drive-cycle and the data available from the Lithium Polymer cell, the temperature rise at the end of a drive-cycle is calculated. This temperature rise is utilized to calculate the improvement in cell operating temperature and thus increase in charge/discharge power through self-heating. The ensuing impact on the energy available from the cell is also analyzed. Self-heating is calculated as per the following equation:

$$\Delta T = \int \frac{i^2 \times R}{m \times C} dt \qquad (9)$$

Here, 'ΔT' is the cell temperature rise at the end of any single drive-cycle, 'i' is the instantaneous current-profile, 'R' is the internal cell resistance, 'm' is the mass of the cell (1.01 kg), and 'C' is its specific heat capacity (~1000 J/kg/^{o}C).

4 Results and Discussion

4.1 Battery Level Energy Decline at Lower Temperatures

The energy available from the battery at 25 ^{o}C using data from Fig. 1 and Equation (1) is calculated as 15.2 kWh. As the SOC window is 50%, this gives 7.6 kWh of energy available from the battery. The energy drawn at different temperatures (Fig. 4) is calculated based on data from Fig. 1. Initially, it is assumed that the aggressiveness of the drive-cycle doesn't impact the energy available from the battery pack. Based on data from Table 1 and Figure 4, the minimum temperatures at which the battery is able to meet the energy demands of any drive-cycle can be concluded (Table 3).

Table 3. Minimum Temperatures where Drive Cycle Energy Demands are met (Including 100% RE)

Drive Cycle	FTP	NEDC	UDDS	US06
Energy (kWh)	2.38	1.71	1.56	2.62
Temp. (^{o}C)	-21.6	-25.2	-26.4	-20.4

For the drive-cycle with the highest energy demands (US06), 2.62 kWh, the battery fails to meet them at a higher ambient temperature (-20.4 ^{o}C) than for the other drive-cycles. Thus, for energy considerations, the battery performs well across all drive-cycles up to and above an ambient temperature of -20.4 ^{o}C. These results neglect the fact that regenerative-braking is not permitted by manufacturers below 0 ^{o}C. That would lead to higher energy demand from the battery. The corresponding effects are shown in Table 4.

Table 4. Effect of Regenerative Braking on Energy Required from Battery for Drive Cycles

RE (%)	100		50		0		Max Energy Available from Regenerative-braking (kWh)	Energy Difference per Drive Cycle (%)
Drive Cycle	Energy Req. (kWh)	Min. Temp. (^{o}C)	Energy Req. (kWh)	Min. Temp. (^{o}C)	Energy Req. (kWh)	Min. Temp. (^{o}C)		
FTP	2.38	-21.6	2.84	-19.2	3.30	-17.0	0.92	39
NEDC	1.71	-25.2	1.90	-24.2	2.09	-23.2	0.38	22
UDDS	1.56	-26.4	1.87	-24.4	2.19	-22.6	0.63	41
US06	2.62	-20.4	2.97	-18.6	3.33	-16.8	0.71	27

Table 4 shows variation in the minimum temperatures where four drive-cycles are met for three RE values: 100%, 50% and 0%. It is seen that UDDS which has the lowest energy demand for 100% RE, has the highest deviation between its energy demands (41%) for the three REs, while the NEDC that has least aggressive deceleration values (Tables 1 and 2), has the lowest deviation between its corresponding energy requirements (22%). The FTP has the greatest difference between its minimum temperature values (4.6 ^{o}C) for the three REs evaluated as it spends the highest time amongst the four drive-cycles on braking (equivalent to maximum of 0.92 kWh of energy from regenerative-braking). The battery fails to meet the US06 drive cycle at -16.8 ^{o}C for 0% regenerative-braking.

4.2 Cell Level Power Decline at Lower Temperatures

Based on Eq. 3 and the limiting voltage values (V_{max} from Fig. 1 and V_{min} being 2.9 V) for cell charging and discharge, the charge and discharge profiles for the cell have been calculated for three SOCs (75%, 50% and 25%).

In Fig. 4, it is seen that charging power from regenerative-braking has different values for the cell over the three different SOCs and ambient temperatures. But, the trends, majorly dependent on the internal resistance and maximum cell voltage, are similar. The maximum charging power from regenerative-braking is for 25% SOC and 25 ºC (-1200 W) ambient temperature. The cell is unable to provide any power below 5, -10 and -15 ºC for 75%, 50% and 25% SOC respectively. Thus, for none of the drive-cycles, the cell will be able to meet the charging power requirements below -15 ºC. This leads to no regenerative-power being offered by the cell below that temperature.

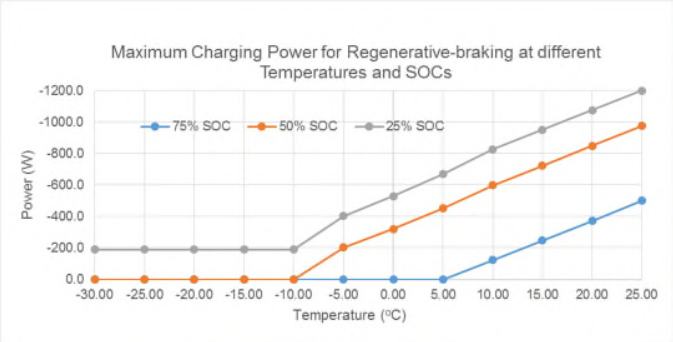

Figure 4. Maximum Power Acceptable by Cell from Regenerative-Braking at Different Temperatures and SOCs

In Fig. 5, discharge power as expected is lowest for 25% SOC and highest for 75% SOC. The US06 drive-cycle has a maximum discharge power of 1261.3 W (Table 2). The battery does not meet this requirement below -22.5 ºC for 75% SOC but the corresponding values for 50% and 25% SOC are -5 and -15 ºC respectively. The cell is able to meet the discharge power requirements of the other three drive-cycles for all SOCs and ambient temperatures. Thus, the SOC and in turn the energy demanded for a particular drive-cycle has a significant impact on the power available from the cell/battery and vice-versa.

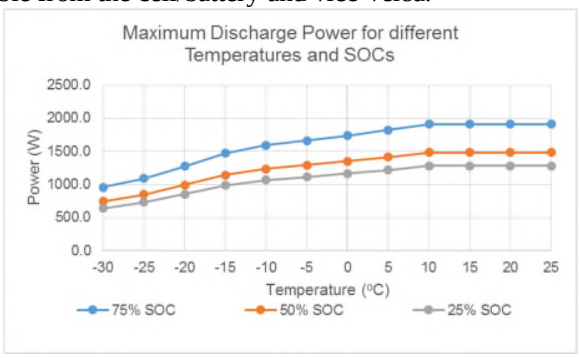

Figure 5. Maximum Discharge Power Offered by Cell at Different SOCs and Temperatures

Since, it is challenging to conclusively predict the minimum temperatures at which the battery is able to meet the power demands (either charge/discharge) of the different drive-cycles, the above data is fed into a MATLAB/Simulink model to dynamically predict that temperature encompassing all SOC points and both charging and discharge operations. This takes into consideration that charge/discharge pulses might occur at any point during a particular drive-cycle and that the SOC might be variable. For this analysis, two regenerative-

braking efficiencies (REs) have been considered, viz. 50% and 0%. Further, this method takes into consideration the energy demanded in each drive-cycle and is thus more realistic.

Table 5. Minimum Temperatures where Battery meets Drive Cycle for Various REs

Drive Cycle	Min. Temp. for 100% RE (ºC)	Min. Temp. for 50% RE (ºC)	Min Temp. for 0% RE (ºC)
FTP	-1.2	-4.2	-30.0
NEDC	-8.4	-12.8	-30.0
UDDS	-8.3	-12.4	-30.0
US06	2.2	-2.4	-12.1

Based on Table 1 and Figures 4 & 5, it can be seen in Table 5, that the FTP, NEDC and UDDS can be met by the battery from a power standpoint till -30 ºC for 0% RE. But, the US06 is not met for 0% RE at temperatures below -12.1 ºC. Based on the aggressiveness of the drive-cycles, the power demands of none of the drive-cycles can be met below -12.8 ºC and -8.4 ºC for 50% and 100% RE respectively. Thus, considering both energy and power demands of the four drive-cycles, for 0%, 50% and 100% REs, Table 6 can be summarized where 'MinE' is the minimum temperature at which the battery is able to meet a particular drive-cycle's energy requirements whereas 'MinP' is the corresponding value for its power demands.

It is seen in Table 6, that US06 is the worst affected by the low temperature performance of Lithium-ion batteries. This can be attributed to its aggressiveness (high charge/discharge power) and greater energy demands. Table 6 concludes that a battery is limited from a power perspective at higher ambient temperature than it is for energy. Table 4 indicates that greater regenerative-braking leads to more severe power decline at lower temperatures. But, Table 3 shows that to improve the energy performance of batteries for different drive-cycles at lower temperatures, greater regenerative-braking is ideal. Although, battery-charging including regenerative-braking is not recommended by manufacturers below 0 ºC, it is seen in Table 6, that above certain temperatures (above -8.3 ºC) and for particular drive-cycles (NEDC and UDDS), regenerative-braking is mathematically possible and has the potential to improve the driving range considerably (From Table 4, by 22% and 41% respectively).

Table 6. Minimum Temperatures where Drive-cycles Energy and Power demands are met for various REs

Drive Cycle	FTP	NEDC	UDDS	US06
MinE (ºC)	-19.2	-24.2	-24.4	-18.6
MinP for 0% RE (ºC)	-30.0	-30.0	-30.0	-12.1
MinP for 50% RE (ºC)	-4.2	-12.8	-12.4	-2.4
MinP for 100% RE (ºC)	-1.2	-8.4	-8.3	2.2

4.3 Impact of Self-heating on Battery Performance

Table 7. Self-heating at Different Ambient Temperatures

Ambient Temperature (ºC)		10	0	-10	-20	-30
FTP	Temperature Rise (ºC)	1.21	1.35	1.49	1.91	2.61
	Self-Heating (kWh)	0.04	0.04	0.04	0.05	0.07
	Energy Lost (%)	1.3	1.4	1.5	1.9	2.5
NEDC	Temperature Rise (ºC)	0.85	0.93	1.01	1.27	1.69
	Self-Heating (kWh)	0.03	0.03	0.03	0.04	0.05
	Energy Lost (%)	1.3	1.4	1.6	2.0	2.6
UDDS	Temperature Rise (ºC)	0.73	0.81	0.88	1.10	1.47
	Self-Heating (kWh)	0.02	0.02	0.03	0.03	0.04
	Energy Lost (%)	1.2	1.3	1.4	1.7	2.3
US06	Temperature Rise (ºC)	2.95	3.25	3.55	4.43	5.91
	Self-Heating (kWh)	0.09	0.10	0.11	0.13	0.18
	Energy Lost (%)	2.9	3.3	3.5	4.4	5.9

In Table 7, for a single drive-cycle, self-heating and battery operating temperature rise has been calculated for the four drive cycles at various ambient temperatures. Here, RE is taken as 50%. Further, cell internal resistance is assumed to remain constant over each single drive-cycle and has been considered for the initial ambient temperature. In Table 6, it is seen that the US06 being the most aggressive drive-cycle shows greater self-heating and corresponding battery operating temperature rise. However, it loses the greatest available to self-heating. At -30 ºC, the battery operating temperature after a single US06 drive-cycle is -24.1 ºC, a rise of 5.91 ºC. This will result in gain in battery power. But, the energy lost to self-heating is 5.9% of the total energy required by the drive-cycle (2.97 kWh). Whereas at 10 ºC for the UDDS only 1.2% of total energy required by the drive-cycle is lost to self-heating to raise the battery operating temperature by 0.73 ºC. The battery loses energy that can be utilized to meet drive-cycle energy demands to increase its operating temperature with the goal to increase power performance. This interdependence and any associated benefit depends upon the drive-cycle.

5 Conclusions

- The Battery is unable to meet the power demands of particular drive cycle at higher temperatures than for corresponding energy requirements. The aggressiveness of the drive cycle increases this temperature difference.
- Greater regenerative-braking leads to more severe battery power decline at lower temperatures. Increased regenerative-braking improves the low temperature energy performance of batteries.
- Regenerative-braking even at subzero ambient temperatures should be employed for particular SOC ranges to improve energy performance of the battery. The C-rate flow into and out of battery determines its performance in terms of energy and power.

- Self-heating can be used as a method to improve battery power performance at lower ambient temperatures. But, this leads to potential loss in driving-range (available energy).
- Both regenerative-braking and self-heating as means to improve the low-temperature energy and power performance are dependent on the levels of current being drawn in and out of the battery. Regenerative-braking power should be limited based on the maximum current that can be drawn into the cell/battery based on the operating temperature and SOC.

6 Further Work

- Analyzing temperature and SOC dependence of regenerative-braking and potential usage of high-power devices (Pulse-batteries or Supercapacitors) to increase its efficiency.
- Quantifying interdependence of battery self-heating and regenerative-braking and their impact on the energy and power performance.

Acknowledgements

The research presented within this paper is supported by the UK Technology Strategy Board (TSB) through the WMG centre High Value Manufacturing (HVM) Catapult in collaboration with Jaguar Land Rover and TATA Motors.

References

1. Chan, C.C., The State of the Art of Electric, Hybrid, and Fuel Cell Vehicles. Proceedings of IEEE, 2007. 95(4).
2. Conte, F.V., Battery and Battery Management for Hybrid Electric Vehicles: A Review. Elektrotechnik und Informationstechnik 2006. 123(10): p. 424-431.
3. Miller, P., Automotive Lithium-Ion Batteries. Johnson Matthey Technology Review, 2015. 59(1): p. 4-13.
4. Miller, J., Energy Storage System Technology Challenges facing Strong Hybrid, Plugin and Battery Electric Vehicles in IEEE. 2009.
5. Jaguemont, J., et al., Low Temperature Discharge Cycle Tests for a Lithium Ion Cell, in IEEE Vehicle Power and Propulsion Conference. 2014: Coimbra.
6. Zhang, Y., C.-Y. Wang, and X. Tang, Cycling degradation of an automotive LiFePO4 lithium-ion battery. Journal of Power Sources, 2011. 196: p. 1513-1520.
7. Keil, P. and A. Jossen, Improving the Low-Temperature Performance of Electric Vehicles by Hybrid Energy Storage Systems, in IEEE Vehicle Power and Propulsion Conference (VPPC). 2014.
8. Zahabi, S.A.H., et al., Fuel economy of hybrid-electric versus conventional gasoline vehicles in real-world conditions: A case study of cold cities in Quebec, Canada. Transportation Research Part D, 2014. 32: p. 184-192.
9. Cho, H.-M., et al., A study on time-dependent low temperature power performance of a lithium-ion battery. Journal of Power Sources, 2012. 198.
10. Jaguemont, J., L. Boulon, and Y. Dubé., Characterization and Modeling of a Hybrid Electric Vehicle Lithium – Ion Battery Pack at Low Temperatures. IEEE Transactions on Vehicular Technology, 2015.

11. Ji, Y. and C.Y. Wang, Heating strategies for Li-ion batteries operated from subzero temperatures. Electrochimica Acta, 2013. 107: p. 664-674.
12. Zhang, S.S., K. Xu, and T.R. Jow, The Low Temperature Performance of Li-ion Batteries. Journal of Power Sources, 2003. 115: p. 137-140.
13. Ji, Y., Y. Zhang, and C.-Y. Wang, Li-Ion Cell Operation at Low Temperatures. Journal of Electrochemical Society, 2013. 160(4): p. 636-649.
14. Senyshyn, A., et al., Low-temperature Performance of Li-ion Batteries: The Behavior of Lithiated Graphite. Journal of Power Sources, 2015. 282: p. 235-240.
15. Burke, A.B., M. Miller, The Power Capability of Ultracapacitors and Lithium Batteries for Electric and Hybrid Vehicle Applications. Journal of Power Sources, 2011. 196: p. 514-522.
16. Waag, W., S. Käbitz, and D.U. Sauer, Experimental Investigation of the Lithium-ion Battery Impedance Characteristic at Various Conditions and Ageing States and its Influence on the Application. Applied Energy, 2013. 102: p. 885-897.

Authors

Yashraj Tripathy holds a B.Eng. (Honours) in Mechanical Engineering from Birla Institute of Technology & Science, Pilani, India. He is currently pursuing a PhD in 'Hybridisation of Energy Storage for High-power Vehicular Applications' as part of the Energy and Electrical Systems group at WMG, University of Warwick. His current field of research is the low-temperature and high C-rate performance of Lithium-ion batteries and Supercapacitors.

Dr Andrew McGordon joined WMG in May 2005, working on the Premium Automotive Research and Development Hybrid Vehicle projects and developed the hybrid powertrain simulation tool, WARPSTAR. He is currently a Principal Engineer in the Energy Storage and Management group at WMG, working on energy storage and vehicle modelling. His current focus is on the modelling of energy storage systems for real world vehicle applications.

Dr John Low is Assistant Professor specialising in Energy for Low Carbon Vehicles. He has previously worked at the Electrochemical Engineering Laboratory and as part of the Energy Technology Research Group at the University of Southampton. He was trained as a Chemical Engineer (Bath University, BEng Chemical Engineering with one-year spent in industrial training, 2000-2004), then Electrochemist (Southampton University, PhD, 2004-2007) and later Electrochemical Engineer (Southampton University, Research Fellow, 2007-2013).

Dr James Marco is a Chartered Engineer and a member of the Institution of Engineering and Technology (IET). After graduating with an Engineering Doctorate, James worked for several years within the automotive industry on a number of different projects including those involving Ford (North America and Europe), Jaguar Cars, Land Rover and Daimler Chrysler. He is currently employed as an Associate Professor in Vehicle Electrification and Energy Storage at WMG, University of Warwick.